The 2018 World Congress on
Advances in Civil, Environmental, & Materials Research (ACEM18)
Songdo Convensia, Incheon, Korea, August 27 - 31, 2018

Seismic performance of two-story wooden house based on structure damage in the 2016 Kumamoto Earthquake

*Tomiya Takatani[1] and Hayato Nishikawa[2]

[1] *Department of Civil Engineering and Architecture, NIT, Maizuru College, Japan*
[2] *Department of Civil Engineering, Fukui Institute of Technology, Fukui, Japan*
[1] *takatani@maizuru-ct.ac.jp*

ABSTRACT

2.2% of wooden houses built after 2000 by the new earthquake resistant design code in Japan was destroyed by the 2016 Kumamoto Earthquake. One of several destruction and collapsing reasons for these wooden houses may be an insufficient strength or a construction failure at junction metallic material between timber elements. In this paper, the effect of the strength of junction metallic material on seismic performance of wooden house is numerically investigated by 3-D collapsing process analysis. The wooden house used in this seismic collapsing analysis against the 2016 Kumamoto Earthquake was built in 2002.

1. INTRODUCTION

So far the Building Standards Act in Japan has been amended several times based on the building damages due to some major earthquakes. Recently, twice large amendments in the Building Standards Act conducted in both 1981 and 2000, and the earthquake resistant design of a Japanese-style wooden house has been much stronger than before. A tremendous seismic damage of collapse to wooden houses was caused by the 2016 Kumamoto Earthquake occurred on both April 14 and 16 (Building Research Institute, 2016). In particular, Mashiki town located at near the hypocenter of these earthquakes has twice earthquake ground motions with the Japan Meteorological Agency (hereafter referred as JMA) seismic intensity of “7” level successively. According to several seismic damage reports on 1,955 wooden structures in Mashiki town, wooden houses with no seismic damage were 414, ones with slight, small and medium seismic damage were 1,014, ones with large seismic damage were 230 and ones with collapse were 297. Especially, wooden houses built before 1981 were 214, ones built from 1981 to 2000 were 76, and ones built after 2000 were 7 from a view point of collapse (National Institute for Land and Infrastructure Management, 2016).

---

[1] Professor
[2] Associate Professor

Takatani and Nishikawa (2014, 2015, 2016, 2017) have been reported the seismic performance of Japanese-style wooden house against several strong earthquake ground motions observed by the national Institute for Earth Science and Disaster Resilience in Japan. However, seismic performance of wooden house against twice strong earthquake ground motions with the JMA seismic intensity of “7” level like the 2016 Kumamoto Earthquake has not been analyzed before. In this paper, 3-D seismic collapsing process analysis (Nakagawa and Ohta, 2010) of the wooden house against the 2016 Kumamoto Earthquake ground motions with the JMA seismic intensity of “7” level was carried out in order to numerically investigate the seismic performance of Japanese-style two-story wooden house. Previously mentioned, 2.2% of wooden houses built after 2000 by the new earthquake resistant design code in Japan was destroyed by the 2016 Kumamoto Earthquake. One of several destruction reasons for these wooden houses may be an insufficient strength or a construction failure at junction metallic material between timber elements. The effect of the strength of junction metallic material on seismic performance of wooden house is numerically investigated by 3-D collapsing process analysis. The wooden house used in this seismic collapsing analysis against the 2016 Kumamoto Earthquake was built in 2002.

2. SEISMIC DAMAGE OF WOODEN STRUCTURE IN THE 2016 KUMAMOTO EARTHQUAKE

Fig.1 shows three epicenter locations of the 2016 Kumamoto Earthquake on April 14 - 16. The 2016 Kumamoto Earthquake caused severe damage to Kumamoto area. Because of the shallow depth of hypocenter, the severe damage was caused in Mashiki town located 10km away from Kumamoto city. The earthquake consists of two

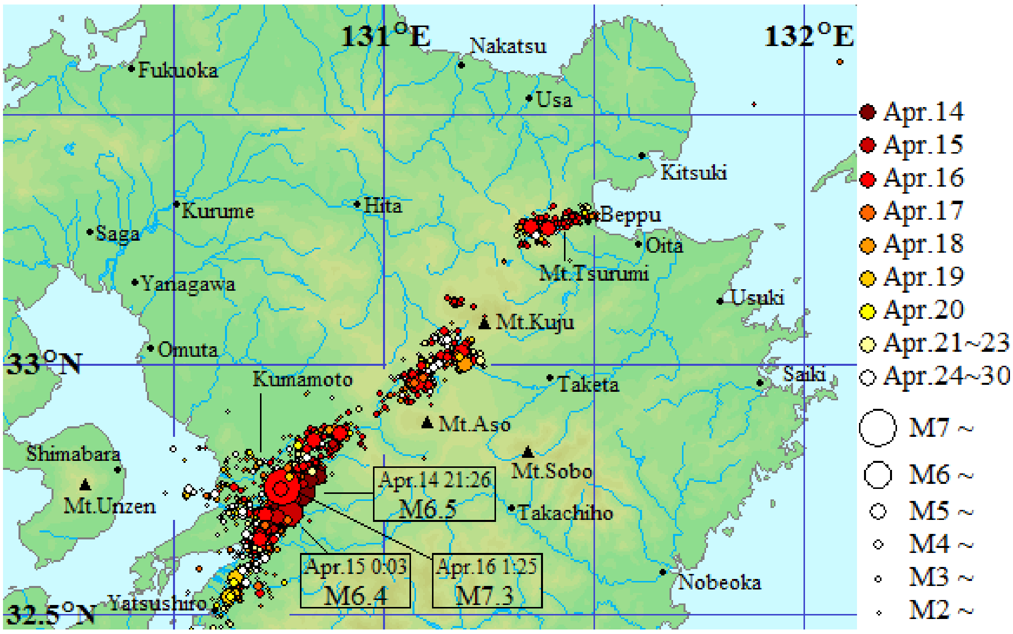

Fig.1 Epicenter locations of the 2016 Kumamoto Earthquake (Wikipedia, 2016).

Table 1 The 2016 Kumamoto Earthquake on both April 14 and April 16.

	Magnitude M	JMA Seismic Intensity	Component	PGA (Gal)	PGV (kine)	PGD (cm)
Foreshock (April 14, 21:26)	6.5	6.5	EW	922.9	90.7	14.9
			NS	759.4	74.6	12.2
			UD	1,399.4	56.1	2.7
Main shock (April 16, 01:25)	7.3	6.5	EW	1,155.8	137.9	38.7
			NS	651.8	84.2	14.4
			UD	873.4	40.2	12.9

strong earthquake ground motions on April 14 and 16 and a series of smaller fore-shocks and aftershocks. The first earthquake with the magnitude 6.5 and the hypocenter depth 10km occurred in the Kumamoto area at 9:26pm, April 14. The acceleration waves measured at Mashiki town during this earthquake are shown in Fig.2. Also, the earthquake with the magnitude 6.4 occurred again in the same area at 0:03am, April 15. The earthquake at 1:25am on April 16 was designated as the main shock of the 2016

Fig.2 indicates seismic damage of wooden structures in Mashiki town on each construction period by exhaustive survey conducted by the National Institute for Land and Infrastructure Management (2016). It is found that there is a significant damage rate of wooden house built before the New Seismic Design Standards Act in Japan amended after 1981 in comparison with that after 1981. Seismic damage of wooden house built after 2000 is quite smaller than that after 1981 because of the specification of joint and connecting metals, balance calculation of seismic wall arrangement for

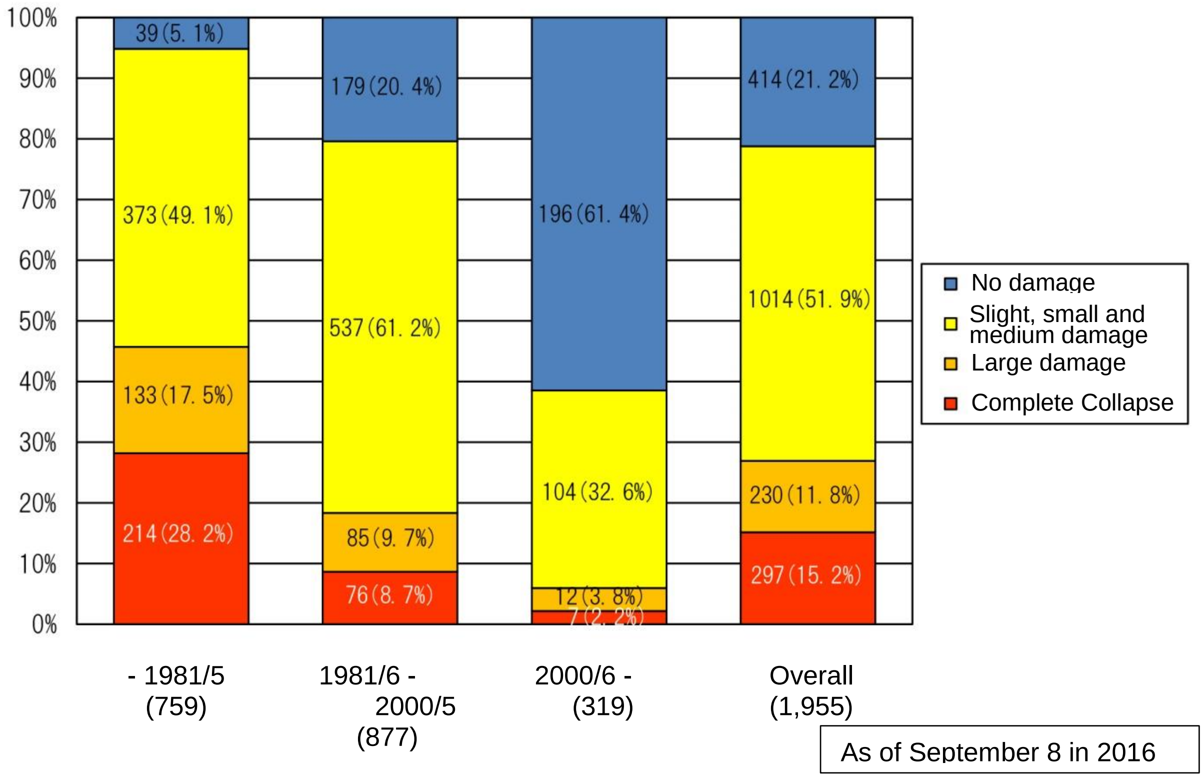

Fig.2 Seismic damage of wooden structures on each construction period by exhaustive survey (National Institute for Land and Infrastructure Management, 2016).

wooden house. In 7 wooden houses built after 2000, 3 wooden houses collapsed because of the insufficient strength at the junction between timber pillar and beam due to some construction failures, and other wooden houses collapsed because of the collapse and inclination of their foundations.

On the other hand, the National Institute for Land and Infrastructure Management (2016) reported that the effect of the reginal seismic coefficient Z was not clearly identified in the seismic damage of wooden house in Mashiki town. The regional seismic coefficient Z in the Building Standards Act in Japan is defined to be a numerical value of 0.7 to 1.0 according to the past seismic damage, seismic fault activities and other seismic state in the area subjected to seismic evaluation. Therefore, the regional seismic coefficient Z in the Kumamoto prefecture has 0.8 to 0.9 because of past seismic damage and fault activities. Because a wooden house built in the Kumamoto prefecture has a lower seismic performance against a strong earthquake in comparison with other region in Japan with high potential for seismic damage and fault activities, they say that there was a tremendous seismic damage of collapse to wooden houses in the Kumamoto prefecture.

3. SEISMIC PERFORMANCE ANALYSIS OF WOODEN HOUSE AGAINST THE 2016 KUMAMOTO EAETHQUAKE

3.1 Transition of the Building Standards Act in Japan

In this section, the transition of the Building Standards Act in Japan is described briefly.

Table 2 shows a transition of the Building Standards Act in Japan since 1920. The Building Standards Act in Japan has been frequently amended based on the building damage due to a major earthquake. After the Kanto Earthquake (M7.9) in 1923, the Urban Area Building Standards Act in Japan has been significantly amended in 1924, and new Seismic Design Standards Act has been enforced in 1981 after the Miyagi-ken Oki Earthquake (M7.4) in 1978. Since 1981, wooden house has been built under a wall quantity regulation condition. The effectiveness of this wall quantity regulation for wooden house was proved in the Hyogo-ken Nanbu Earthquake (M7.3) in 1995. A lot of wooden houses built before 1981 were destroyed by this earthquake, while almost wooden houses built by the New Seismic Design Standards Act in Japan after 1981 did not collapse. After the Hyogo-ken Nanbu Earthquake in 1995, the Building Standards Act in Japan has been amended in 1995 so as to use the joint and connecting metals at the connection point between wooden frame members. The Building Standards Act has been amended in 2000, and the mandatory of ground investigation, the specification of joint and connecting metals, and the balance calculation of seismic wall arrangement in wooden house were conducted after 2000. Moreover, seismic retrofit for wooden house built before 1981 has been strongly promoted in 2006 in order to reduce seismic damage of wooden house with a low seismic performance against a strong earthquake ground motion.

In 2016, the Kumamoto Earthquake (M7.3) occurred on April 16 after a foreshock earthquake (M6.5) occurred on April 14. A lot of buildings over 100,000 were damaged

Table 2 Transition of Seismic Design Standards on Wooden Structure

Year	Details of Transition
1920	The Urban Area Building Standards Act Enforcement (New Building Standard Act in Japan)
1924	Significant Amendment of the Urban Area Building Standards Act (Seismic Intensity Design)
1950	Establishment of the Building Standards Act (Wall Quantity Regulation, Allowable Stress Design method)
1959	Amendment of the Building Standards Act (Fire-proof Regulation, Strengthening of Wall Quantity Regulation)
1971	Amendment of the Building Standards Act Enforcement Order (Wooden House Foundation Regulation: Concrete or RC Strip Footing)
1981	Significant Amendment of the Building Standards Act Enforcement Order (New Seismic Design Standards Act, Overhaul of Wall Quantity Regulation)
1987	Amendment of the Building Standards Act (The Lifting of the Ban of Three-story Wooden House Construction)
1995	Amendment of the Building Standards Act (Encouragement of Joint Metal or Hardware between Frame members)
2000	Amendment of the Building Standards Act (Mandatory of Ground Investigation, Specification of Joint and Connecting Metals, Balance Calculation of Seismic Wall Arrangement)
2006	Modified Seismic Retrofit Promotion Act (Promotion of Intentional Seismic Retrofit, Strengthening of Guidance for Building, Expansion of Financial Supporting Action)

by twice strong earthquakes, and so many wooden houses in Mashiki town were destroyed, where was experienced the JMA seismic intensity of “7” level twice. It was found that 17 wooden houses built after 2000 may be collapsed by two earthquake motions on both April 14 and 16. Seismic damage of wooden house may be caused by the weak ground, the construction stage, and the insufficiency of seismic performance. At the present time, the seismic design of a wooden house is not conducted not to collapse against twice strong earthquake motions with the JMA seismic intensity of “7” level under the Building Standards Act in Japan. Therefore, seismic design regulation in the Building Standards Act in Japan would be a possibility to be amended in near future.

3.2 Input Earthquake Motion Waves in the 2016 Kumamoto Earthquake

Fig. 3 shows 11 location points in the Kumamoto prefecture, and 11 earthquake motion waves have JMA seismic intensity of “6+” level and were observed on April 16, 2016 (JMA, 2016). In this paper, 11 earthquake motion waves are employed in seismic performance evaluation of wooden house by 3-D collapsing process analysis.

Fig. 4 indicates Fourier spectra of three components of earthquake acceleration waves observed at location point of “A” shown in Fig. 3, and also three displacement waves calculated from acceleration waves are illustrated in Fig. 4. These displacement waves are employed in 3-D seismic collapsing process analysis of wooden house.

Table 3 shows maximum acceleration values in three components and seismic in-

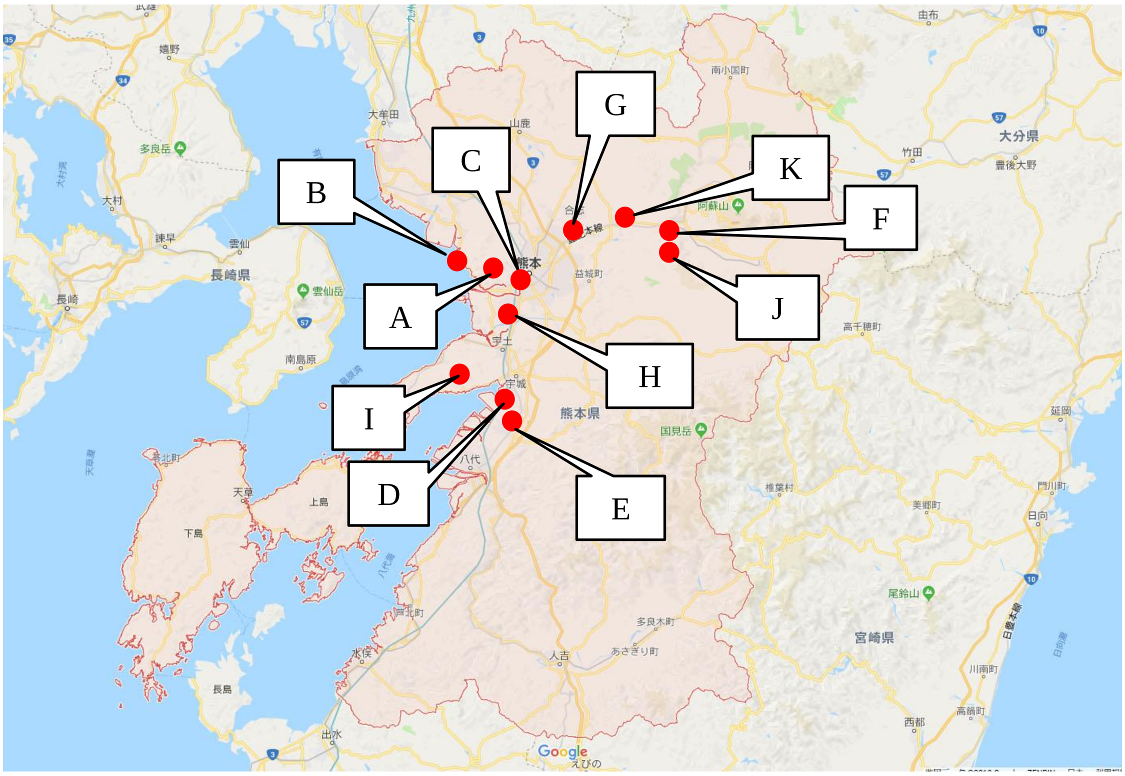

Fig.3 Earthquake motion observation locations

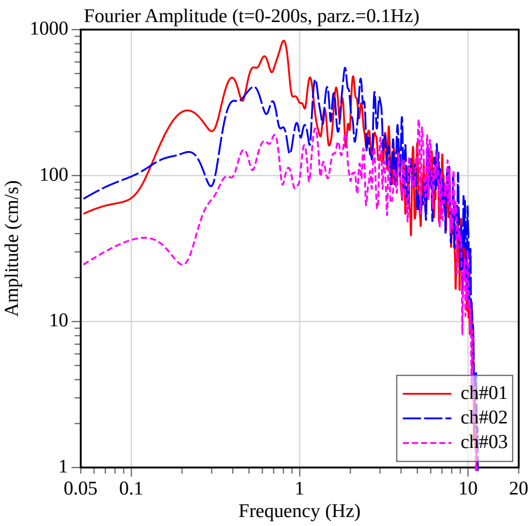

(a) Fourier spectra

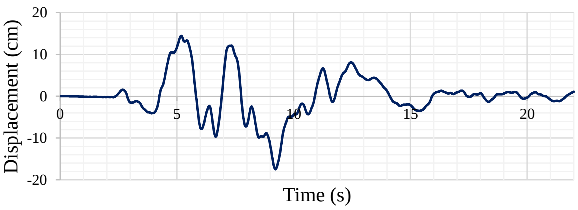

(b) Displacement wave (NS component)

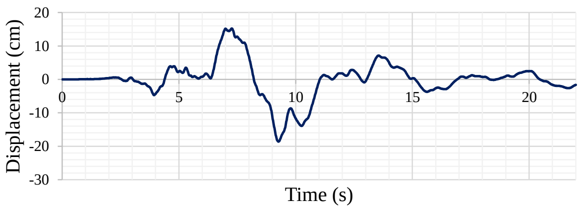

(c) Displacement wave (EW component)

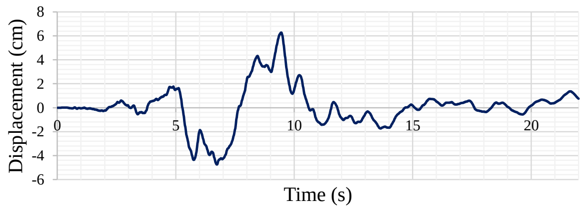

(d) Displacement wave (UD component)

Fig. 4 Fourier spectra and displacement waves at location point A

Table 3 Maximum acceleration values at 11 location points

Location point	Maximum acceleration (Gal)			
	NS	EW	UD	Seismic Intensity
A	606.0	551.6	405.3	6.0
B	492.8	342.6	313.9	6.0
C	626.9	478.2	403.4	6.0
D	389.8	369.4	233.4	6.0
E	573.4	575.1	724.7	6.1
F	1,379.6	1,740.1	594.7	6.1
G	398.8	690.8	306.6	6.2
H	564.8	597.1	474.1	6.2
I	572.0	792.4	466.2	6.2
J	1,111.8	954.6	654.4	6.2
K	799.2	857.4	535.8	6.4

Table 4 Predominant peak frequencies of NS and EW components

Location point	Peak frequency (Hz)	
	NS	EW
A	0.803	1.859
B	0.659	1.215
C	1.642	1.215
D	0.415	0.671
E	1.453	1.111
F	2.979	2.856
G	1.953	1.917
H	0.635	1.282
I	0.755	1.404
J	2.625	1.831
K	1.416	1.196

tensities at 11 local points shown in Fig. 3.

Table 4 shows predominant peak frequencies of NS and EW components of acceleration waves observed at 11 location points, which were obtained from Fourier spectra of acceleration waves. In this paper, the effect of the peak frequency of acceleration wave on the seismic performance of wooden house is numerically investigated.

3.3 Outline of Wooden House and Its Collapsing Model

Target of the collapsing process analysis in this paper is a two-story wooden house, which was built by a traditional wood framed-based construction method in 2002.

The seismic collapsing model is shown in Fig.5, and the model with roof joist elements is indicated in Fig.5(a) and the model with walls, braces, and roof joists is illustrated in Fig.5(b).

In the collapsing analysis of this wooden house shown in Fig.5, the characteristics of these joint metals previously mentioned are modeled by some non-linear load-displacement relationships. However, these non-linear load-displacement relationships between timber pillar and beam elements and the seismic collapsing process analysis of "wallstat" software (Nakagawa and Ohta, 2010) based on the Discrete Element Method proposed by Cundall and Strack (1979) are not indicated due to the limited space.

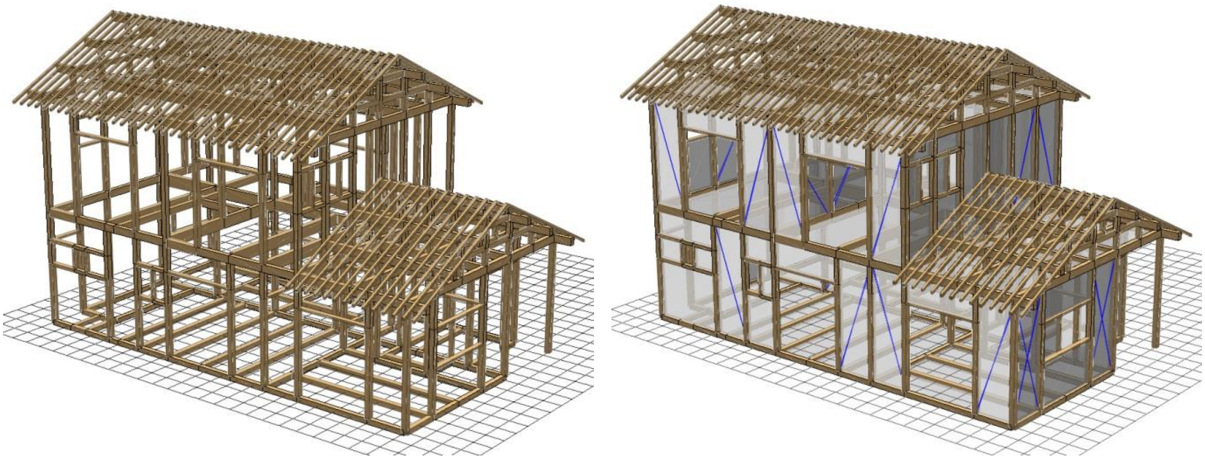

(a) With roof joist (b) With roof joists, walls and braces

Fig.5 Framing model with roof joist of two-story wooden house

In this paper, the maximum drift angle during a strong earthquake motion is numerically evaluated by 3-D collapsing process analysis. Fig. 6 indicates two timber pillars on wooden house, and the effect of the maximum drift angle at each timber pillar on seismic performance of wooden house is investigated.

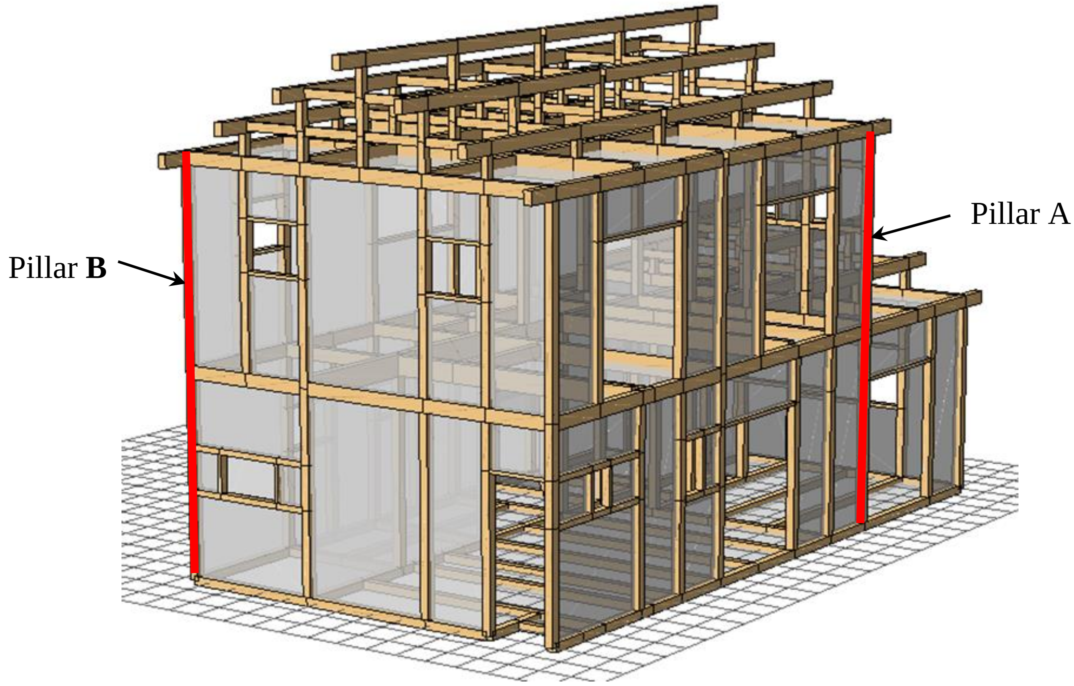

Fig.6 Framing model two-story wooden house

3.4 Seismic Collapsing Results on Maximum Drift Angle

(a) The effect of junction metal material

The effect of junction metallic material on seismic performance of wooden house is investigated. Table 5 shows the maximum drift angles of both first floor and second one of wooden house in X and Y directions on Pillar A indicated in Fig.6. In 3-D seismic collapsing process analysis, EW component was employed in X direction and NS one was done in Y direction of wooden house. These maximum drift angles were obtained from seismic behavior of Pillar A in wooden house during each earthquake motion wave. It is found from Table 5 that the maximum drift angle of the first floor of wooden house with junction metallic materials is almost the same as that of wooden house without junction metallic materials for each earthquake motion wave. On the other hand, the maximum drift angle of the second floor of wooden house without junction metallic materials is larger than that of wooden house with junction metallic materials and the junction metallic material has a great effect on the maximum drift angle response. This is because that the effect of the junction metallic material in wooden house on the maximum drift angle of the first floor was not large because of a strong earthquake motion wave with JMA seismic intensity of “6+” level. However, junction metallic material has a tendency to decrease the maximum drift angle of the second floor of wooden house and also has an effective seismic performance of wooden house.

Table 5 Maximum drift angle at Pillar A
(NS component in X direction and EW component in Y direction)

Location point	First floor				Second floor			
	X direction		Y direction		X direction		Y direction	
	With	Without	With	Without	With	Without	With	Without
A	0.0673	0.0666	0.0660	0.0671	0.0044	0.0026	0.0027	0.0043
B	0.0414	0.0416	0.0959	0.0974	0.0016	0.0015	0.0011	0.0012
C	0.0832	0.0829	0.0786	0.0789	0.0018	0.0023	0.0034	0.0035
D	0.0643	0.0645	0.0912	0.0915	0.0010	0.0009	0.0009	0.0008
E	0.0526	0.0526	0.0949	0.0955	0.0041	0.0037	0.0021	0.0019
F	0.0849	0.0856	0.1013	0.1075	0.0053	0.0066	0.0038	0.0039
G	0.1047	0.1044	0.1029	0.1035	0.0016	0.0042	0.0008	0.0022
H	0.0784	0.0780	0.1491	0.1549	0.0019	0.0029	0.0017	0.0027
I	0.0618	0.0638	0.0630	0.0689	0.0025	0.0040	0.0016	0.0018
J	0.1380	0.1386	0.2041	0.2118	0.0045	0.0052	0.0023	0.0055
K	0.0712	0.0705	0.1338	0.1340	0.0043	0.0048	0.0019	0.0045

Table 6 Maximum drift angle at Pillar A
(EW component in X direction and NS component in Y direction)

Location point	First floor				Second floor			
	X direction		Y direction		X direction		Y direction	
	With	Without	With	Without	With	Without	With	Without
A	0.0635	0.0634	0.0688	0.0746	0.0032	0.0033	0.0028	0.0024
B	0.0939	0.0939	0.0420	0.0443	0.0011	0.0014	0.0016	0.0011
C	0.0759	0.0752	0.0872	0.0860	0.0055	0.0046	0.0021	0.0019
D	0.0890	0.0889	0.0642	0.0653	0.0011	0.0010	0.0007	0.0006
E	0.0924	0.0924	0.0576	0.0578	0.0034	0.0025	0.0024	0.0022
F	0.0984	0.0967	0.0883	0.0968	0.0035	0.0061	0.0038	0.0049
G	0.1008	0.1015	0.1081	0.1236	0.0012	0.0068	0.0025	0.0050
H	0.1476	0.1474	0.0796	0.0900	0.0019	0.0030	0.0015	0.0037
I	0.0643	0.0639	0.0659	0.0763	0.0021	0.0024	0.0020	0.0037
J	0.2016	0.1992	0.1389	0.1670	0.0045	0.0103	0.0040	0.0065
K	0.1349	0.1343	0.0755	0.0732	0.0035	0.0055	0.0038	0.0047

While, Table 6 illustrates the maximum drift angles of both first floor and second one of wooden house in X and Y directions on Pillar A indicated in Fig.6. In this 3-D seismic collapsing process analysis, NS component was employed in X direction and EW one was done in Y direction of wooden house. From Table 6, the maximum drift angle of the first floor of wooden house with junction metallic materials is almost the same as that of wooden house without junction metallic materials for each earthquake motion wave. On the other hand, the maximum drift angle of the second floor of wooden house without junction metallic materials is larger than that of wooden house with junction metallic materials and the junction metallic material has a great effect to decrease the maximum drift angle response.

Table 7 shows the maximum drift angles of both first floor and second one of wooden house in X and Y directions on Pillar B indicated in Fig.6. In 3-D seismic collapsing process analysis, EW component was employed in X direction and NS one was done in Y direction of wooden house. These maximum drift angles were obtained from seismic behavior of Pillar B in wooden house during each earthquake motion wave. While, Table 8 illustrates the maximum drift angles of both first floor and second

Table 7 Maximum drift angle at Pillar B
(NS component in X direction and EW component in Y direction)

Location point	First floor				Second floor			
	X direction		Y direction		X direction		Y direction	
	With	Without	With	Without	With	Without	With	Without
A	0.0674	0.0674	0.0663	0.0671	0.0063	0.0057	0.0027	0.0028
B	0.0414	0.0414	0.0946	0.0952	0.0025	0.0032	0.0010	0.0011
C	0.0830	0.0830	0.0765	0.0761	0.0026	0.0046	0.0033	0.0023
D	0.0643	0.0644	0.0905	0.0898	0.0017	0.0018	0.0011	0.0006
E	0.0524	0.0518	0.0945	0.0936	0.0051	0.0067	0.0022	0.0015
F	0.0835	0.0832	0.1037	0.0957	0.0061	0.0095	0.0037	0.0023
G	0.1045	0.1042	0.1020	0.1018	0.0025	0.0065	0.0009	0.0016
H	0.0784	0.0782	0.1484	0.1496	0.0022	0.0040	0.0018	0.0021
I	0.0618	0.0634	0.0632	0.0657	0.0035	0.0083	0.0018	0.0012
J	0.1379	0.1379	0.2021	0.2040	0.0059	0.0078	0.0024	0.0036
K	0.0706	0.0697	0.1341	0.1317	0.0054	0.0116	0.0024	0.0029

Table 8 Maximum drift angle at Pillar B
(EW component in X direction and NS component in Y direction)

Location point	First floor				Second floor			
	X direction		Y direction		X direction		Y direction	
	With	Without	With	Without	With	Without	With	Without
A	0.0635	0.0634	0.0683	0.0699	0.0038	0.0062	0.0683	0.0699
B	0.0936	0.0938	0.0417	0.0424	0.0020	0.0039	0.0417	0.0424
C	0.0756	0.0749	0.0848	0.0838	0.0073	0.0085	0.0848	0.0838
D	0.0889	0.0888	0.0645	0.0645	0.0019	0.0026	0.0645	0.0645
E	0.0924	0.0926	0.0549	0.0522	0.0045	0.0054	0.0549	0.0522
F	0.0964	0.0965	0.0956	0.0847	0.0045	0.0084	0.0956	0.0847
G	0.1009	0.1011	0.1066	0.1147	0.0020	0.0045	0.1066	0.1147
H	0.1475	0.1479	0.0789	0.0827	0.0025	0.0055	0.0789	0.0827
I	0.0643	0.0639	0.0646	0.0686	0.0032	0.0049	0.0646	0.0686
J	0.2010	0.2015	0.1418	0.1536	0.0059	0.0113	0.1418	0.1536
K	0.1341	0.1345	0.0724	0.0715	0.0044	0.0069	0.0724	0.0715

one of wooden house in X and Y directions on Pillar B indicated in Fig.6. In this 3-D seismic collapsing process analysis, NS component was employed in X direction and EW one was done in Y direction of wooden house. From Tables 7 and 8, the maximum drift angle of the first floor of wooden house with junction metallic materials is almost

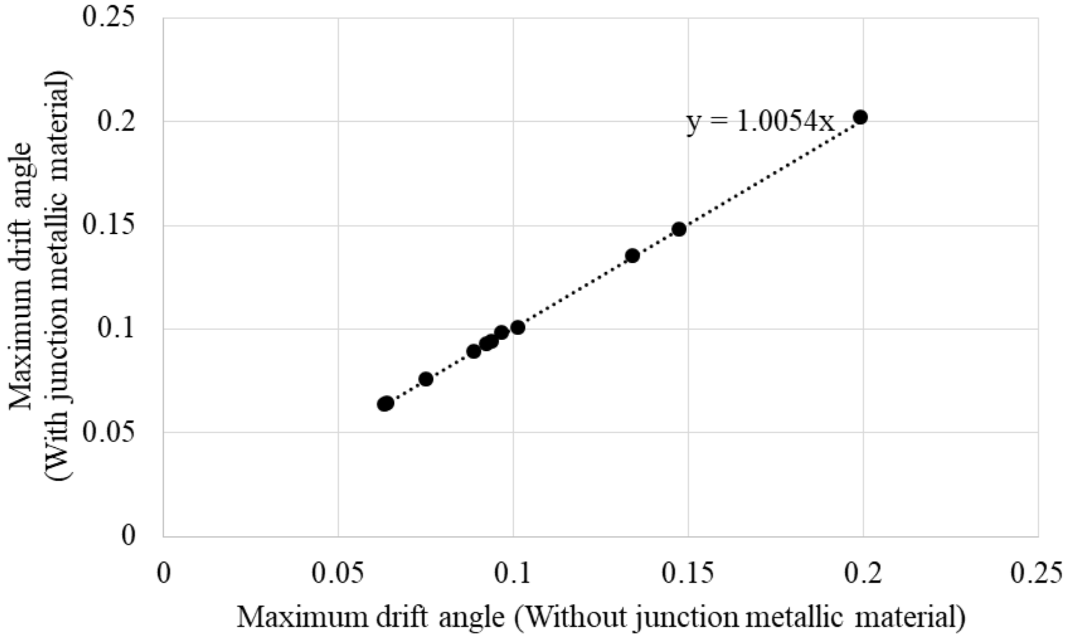

(a) First floor

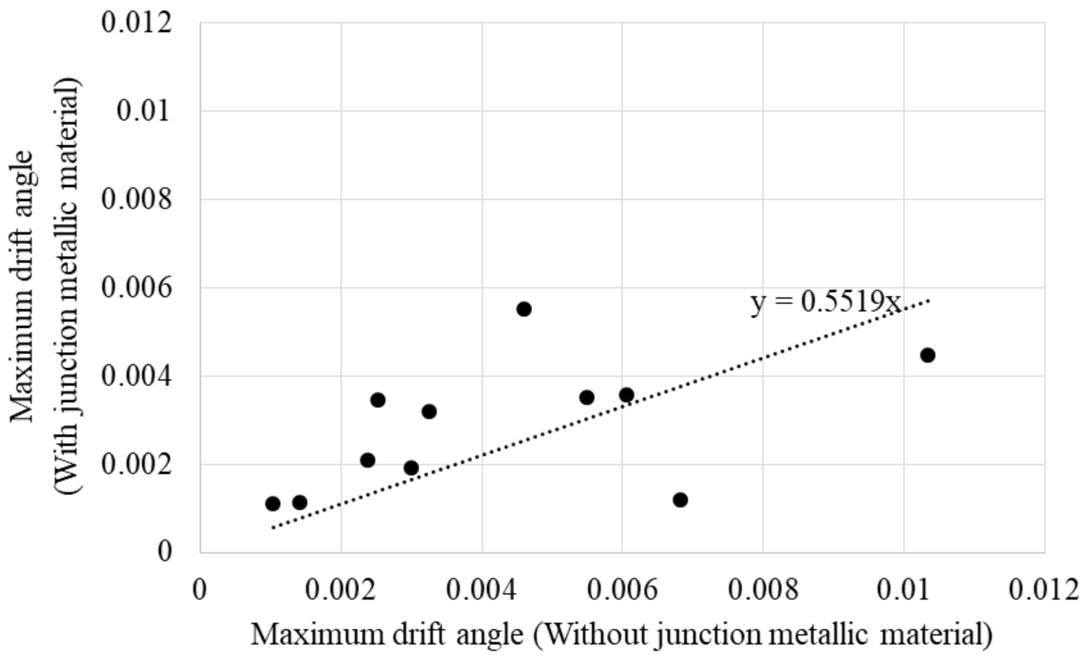

(b) Second floor

Fig. 7 Relationship between maximum drift angle with and without junction metallic material (NS component in X direction and EW component in Y direction) the same as that of wooden house without junction metallic materials for each earthquake motion wave. On the other hand, the maximum drift angle of the second floor of wooden house without junction metallic materials is larger than that of wooden house with junction metallic materials and the junction metallic material has a great

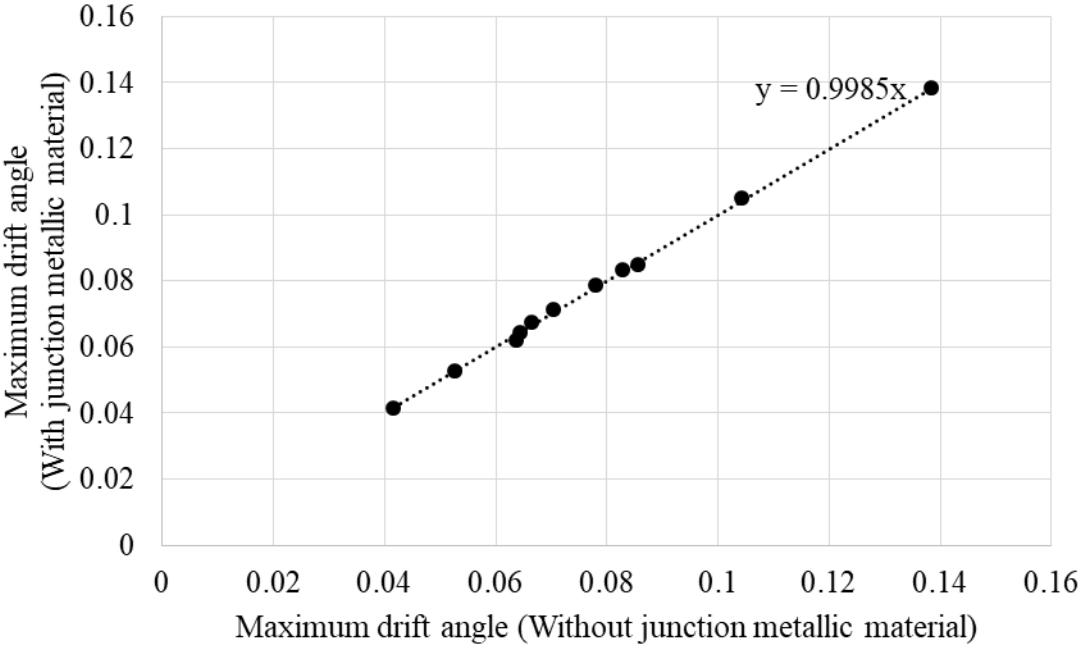

(a) First floor

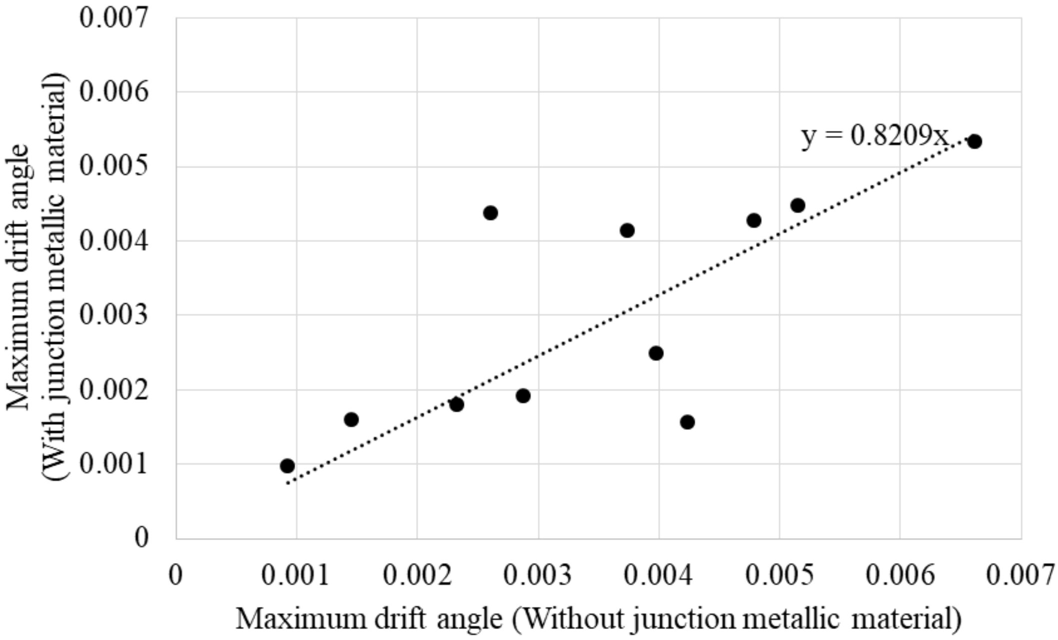

(b) Second floor

Fig. 8 Relationship between maximum drift angle with and without junction metallic material (EW component in X direction and NS component in Y direction) effect on the maximum drift angle response. This is because that the effect of the junction metallic material in wooden house on the maximum drift angle of the first floor was not large because of a strong earthquake motion wave with JMA seismic intensity of “6+” level. However, junction metallic material has a tendency to decrease the maximum drift angle of the second floor of wooden house and also has an effective seismic performance of wooden house.

Fig. 7 shows a relationship between maximum drift angle with and without junction metallic material of wooden house based on the maximum drift angles indicated in Tables 5 and 6. Also, Fig. 7 illustrates a relationship between maximum drift angle with and without junction metallic material of wooden house based on the maximum drift angles indicated in Tables 7 and 8. The maximum drift angle of the first floor of wooden house with junction metallic materials is almost the same as that of wooden house without junction metallic materials for each earthquake motion wave. On the other hand, the maximum drift angle of the second floor of wooden house without junction metallic materials is larger than that of wooden house with junction metallic materials and the junction metallic material has a great effect on the maximum drift angle response. This is because that the effect of the junction metallic material in wooden house on the maximum drift angle of the first floor was not large because of a strong earthquake motion wave with JMA seismic intensity of “6+” level. However, junction metallic material has a tendency to decrease the maximum drift angle of the second floor of wooden house and also has an effective seismic performance of wooden house.

(b) The effect of a construction failure of junction metallic material

The effect of a construction failure of junction metallic material on seismic performance of wooden house is investigated in this session. Watanabe et al.(2003) reported the load and displacement relationship of junction metallic material when the construction is good and poor. According this report by Watanabe et al. (2003), the deformation of wooden house in the poor construction of junction metallic material is almost twice as that in the good construction of junction metallic material. In this paper, the stiffness of junction metallic material in the poor construction is assumed to be half of the good construction.

Table 9 shows the maximum drift angle at Pillar A in both the good and poor construction of junction metallic material for each earthquake motion wave. In 3-D seismic collapsing process analysis, EW component was employed in X direction and NS one was done in Y direction of wooden house. Table 10 indicates the maximum drift angle at Pillar A in both the good and poor construction of junction metallic material for each earthquake motion wave. In 3-D seismic collapsing process analysis, NS component was employed in X direction and EW one was done in Y direction of wooden house. The maximum drift angle of the first floor of wooden house is almost the same as that of wooden house regardless of the good or poor construction condition of junction metallic materials for each earthquake motion wave. On the other hand, the maximum drift angle of the second floor of wooden house under the poor construction condition of junction metallic materials is larger than that of wooden house under the good construction condition of junction metallic materials and the maximum drift angle response greatly depends on the construction condition of junction metallic material. This is because that the effect of the construction condition of junction metallic material in wooden house on the maximum drift angle of the first floor was not large because of a strong earthquake motion wave with JMA seismic intensity of “6+” level. However, the construction condition of junction metallic material has a tendency to decrease the maximum drift angle of the second floor of wooden house and also has an effective seismic performance of wooden house.

Table 11 shows the maximum drift angle at Pillar A in both the good and poor construction of junction metallic material for each earthquake motion wave. In 3-D seismic collapsing process analysis, EW component was employed in X direction and NS one was done in Y direction of wooden house. Table 12 indicates the maximum drift angle at Pillar A in both the good and poor construction of junction metallic material for each earthquake motion wave. In 3-D seismic collapsing process analysis, NS component was employed in X direction and EW one was done in Y direction of wooden house. The maximum drift angle of the first floor of wooden house is almost the same as that of wooden house regardless of the good or poor construction condition of junction metallic materials for each earthquake motion wave. On the other hand, the maximum drift angle of the second floor of wooden house under the poor construction

Table 9 Maximum drift angle at Pillar A
(NS component in X direction and EW component in Y direction)

Location point	First floor				Second floor			
	X direction		Y direction		X direction		Y direction	
	Good	Poor	Good	Poor	Good	Poor	Good	Poor
A	0.0673	0.0673	0.0660	0.0687	0.0044	0.0049	0.0027	0.0022
B	0.0414	0.0414	0.0959	0.0962	0.0016	0.0014	0.0011	0.0011
C	0.0832	0.0832	0.0786	0.0766	0.0018	0.0020	0.0034	0.0031
D	0.0643	0.0644	0.0912	0.0909	0.0010	0.0009	0.0009	0.0007
E	0.0526	0.0525	0.0949	0.0947	0.0041	0.0045	0.0021	0.0020
F	0.0849	0.0853	0.1013	0.1051	0.0053	0.0051	0.0038	0.0039
G	0.1047	0.1051	0.1029	0.1039	0.0016	0.0017	0.0008	0.0010
H	0.0784	0.0788	0.1491	0.1512	0.0019	0.0028	0.0017	0.0023
I	0.0618	0.0619	0.0630	0.0657	0.0025	0.0026	0.0016	0.0016
J	0.1380	0.1384	0.2041	0.2156	0.0045	0.0046	0.0023	0.0042
K	0.0712	0.0713	0.1338	0.1356	0.0043	0.0045	0.0019	0.0023

Table 10 Maximum drift angle at Pillar A
(EW component in X direction and NS component in Y direction)

Location point	First floor				Second floor			
	X direction		Y direction		X direction		Y direction	
	Good	Poor	Good	Poor	Good	Poor	Good	Poor
A	0.0635	0.0631	0.0688	0.0727	0.0032	0.0043	0.0028	0.0026
B	0.0939	0.0940	0.0420	0.0420	0.0011	0.0012	0.0016	0.0014
C	0.0759	0.0762	0.0872	0.0854	0.0055	0.0059	0.0021	0.0019
D	0.0890	0.0892	0.0642	0.0650	0.0011	0.0012	0.0007	0.0007
E	0.0924	0.0926	0.0576	0.0597	0.0034	0.0036	0.0024	0.0024
F	0.0984	0.0984	0.0883	0.0902	0.0035	0.0042	0.0038	0.0046
G	0.1008	0.1009	0.1081	0.1076	0.0012	0.0014	0.0025	0.0029
H	0.1476	0.1479	0.0796	0.0789	0.0019	0.0025	0.0015	0.0017
I	0.0643	0.0640	0.0659	0.0684	0.0021	0.0021	0.0020	0.0026
J	0.2016	0.1990	0.1389	0.1464	0.0045	0.0049	0.0040	0.0042
K	0.1349	0.1338	0.0755	0.0710	0.0035	0.0044	0.0038	0.0044

condition of junction metallic materials is larger than that of wooden house under the good construction condition of junction metallic materials and the maximum drift angle response greatly depends on the construction condition of junction metallic material. This is because that the effect of the construction condition of junction metallic material in wooden house on the maximum drift angle of the first floor was not large because of a strong earthquake motion wave with JMA seismic intensity of “6+” level. However, the construction condition of junction metallic material has a tendency to decrease the maximum drift angle of the second floor of wooden house and also has an effective seismic performance of wooden house.

(c) Relationship between the maximum drift angle and peak frequency of earthquake motion wave

The maximum drift angle of wooden house without junction metallic material is larger than that with junction metallic material in some cases in Tables 5 to 8. This is because that the reinforcement of wooden house by the junction metallic material changes a natural peak frequency of wooden house and its peak frequency may coin-

Table 11 Maximum drift angle at Pillar B
(NS component in X direction and EW component in Y direction)

Location point	First floor				Second floor			
	X direction		Y direction		X direction		Y direction	
	Good	Poor	Good	Poor	Good	Poor	Good	Poor
A	0.0674	0.0674	0.0663	0.0676	0.0063	0.0064	0.0027	0.0025
B	0.0414	0.0414	0.0946	0.0948	0.0025	0.0024	0.0010	0.0010
C	0.0830	0.0830	0.0765	0.0753	0.0026	0.0025	0.0033	0.0028
D	0.0643	0.0644	0.0905	0.0902	0.0017	0.0015	0.0011	0.0008
E	0.0524	0.0521	0.0945	0.0941	0.0051	0.0053	0.0022	0.0020
F	0.0835	0.0835	0.1037	0.1041	0.0061	0.0062	0.0037	0.0034
G	0.1045	0.1047	0.1020	0.1023	0.0025	0.0027	0.0009	0.0012
H	0.0784	0.0786	0.1484	0.1497	0.0022	0.0024	0.0018	0.0020
I	0.0618	0.0620	0.0632	0.0647	0.0035	0.0034	0.0018	0.0019
J	0.1379	0.1381	0.2021	0.2137	0.0059	0.0060	0.0024	0.0036
K	0.0706	0.0706	0.1341	0.1359	0.0054	0.0056	0.0024	0.0024

Table 12 Maximum drift angle at Pillar B
(EW component in X direction and NS component in Y direction)

Location point	First floor				Second floor			
	X direction		Y direction		X direction		Y direction	
	Good	Poor	Good	Poor	Good	Poor	Good	Poor
A	0.0635	0.0633	0.0683	0.0698	0.0038	0.0040	0.0683	0.0024
B	0.0936	0.0937	0.0417	0.0419	0.0020	0.0021	0.0417	0.0013
C	0.0756	0.0757	0.0848	0.0836	0.0073	0.0076	0.0848	0.0018
D	0.0889	0.0891	0.0645	0.0647	0.0019	0.0020	0.0645	0.0006
E	0.0924	0.0924	0.0549	0.0550	0.0045	0.0046	0.0549	0.0022
F	0.0964	0.0966	0.0956	0.0946	0.0045	0.0040	0.0956	0.0038
G	0.1009	0.1010	0.1066	0.1058	0.0020	0.0022	0.1066	0.0030
H	0.1475	0.1478	0.0789	0.0789	0.0025	0.0027	0.0789	0.0019
I	0.0643	0.0644	0.0646	0.0663	0.0032	0.0029	0.0646	0.0024
J	0.2010	0.2008	0.1418	0.1504	0.0059	0.0056	0.1418	0.0039
K	0.1341	0.1340	0.0724	0.0678	0.0044	0.0049	0.0724	0.0034

cide with a predominant peak frequency of the earthquake motion wave.

In this session, a relationship between the maximum drift angle and predominant peak frequency of earthquake motion wave.

Fig. 9 shows a relationship between the maximum drift angle of wooden house and a predominant peak frequency of each earthquake motion wave under the junction metallic material condition. In 3-D seismic collapsing process analysis, EW component was employed in X direction and NS one was done in Y direction of wooden house. Predominant peak frequency in NS component is employed in Fig. 9. Two approximation curves of the maximum drift angle of wooden house with and without

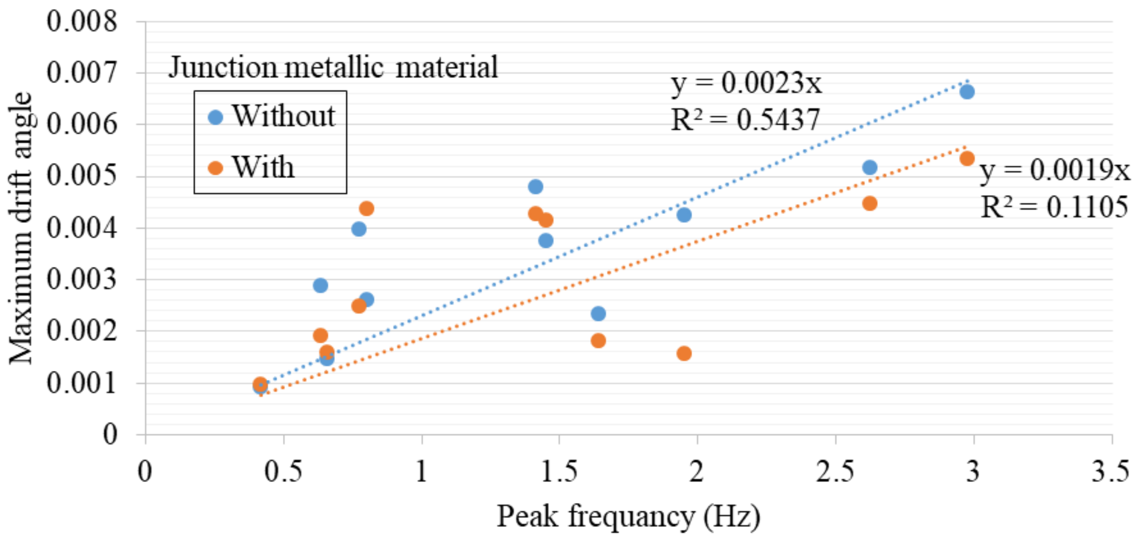

(a) X direction

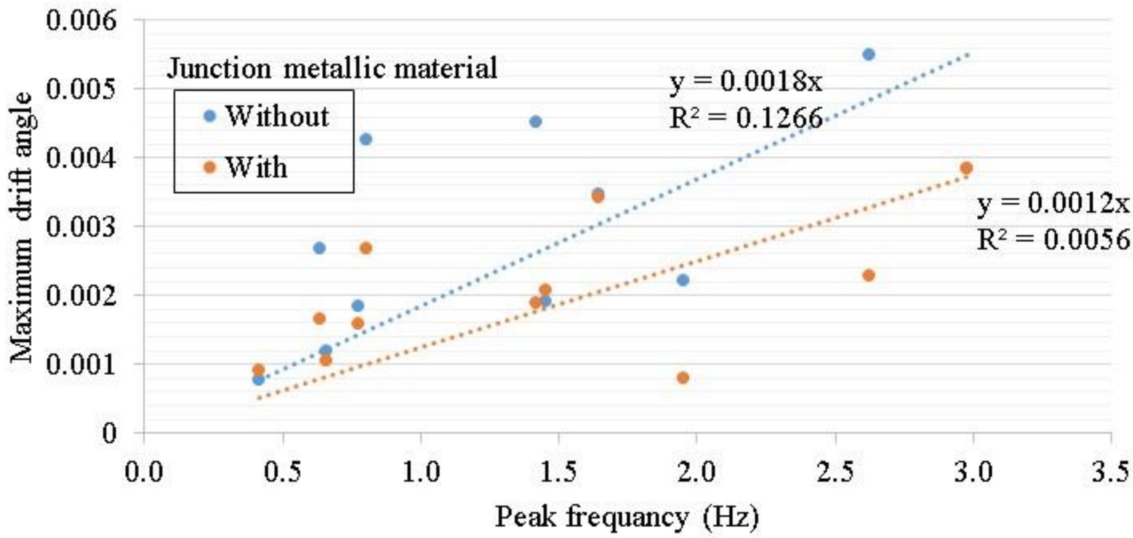

(b) Y direction

Fig. 9 Relationship between maximum drift angle and predominant peak frequency of earthquake motion wave (NS component in X direction and EW component in Y direction) junction metallic material are indicated in Fig. 9. It is found that the approximation curve of the maximum drift angle of wooden house with junction metallic material is smaller than that without junction metallic material. This implies that the deformation of wooden house with junction metallic material is small in comparison with wooden house without junction metallic material. The maximum drift angle of wooden house increases with the predominant peak frequency of earthquake motion wave, and depends on the predominant peak frequency of earthquake motion wave.

4. CONCLUSIONS

In this paper, 3-D seismic collapsing process analysis (Nakagawa and Ohta, 2010) of the wooden house against the 2016 Kumamoto Earthquake ground motions with the JMA seismic intensity of “7” level was carried out in order to numerically investigate the seismic performance of Japanese-style two-story wooden house. 2.2% of wooden houses built after 2000 by the new earthquake resistant design code in Japan was destroyed by the 2016 Kumamoto Earthquake. One of several destruction reasons for these wooden houses may be an insufficient strength at junction metallic material between timber elements. The effect of the strength of junction metallic material on seismic performance of wooden house is numerically investigated by 3-D collapsing process analysis. The wooden house used in this seismic collapsing analysis against the 2016 Kumamoto Earthquake was built in 2002. The summary of this paper is as follows,

1) The maximum drift angle of wooden house trends to increase with a predominant peak frequency of earthquake motion wave and depends on the predominant peak frequency of earthquake motion wave.
2) The effect of the junction metallic material between timber elements on the maximum drift angle of wooden house is much larger in the second floor in comparison with the first floor of wooden house. This is because the existence of junction metallic material is not affected seismic performance in the first floor of wooden house against a strong earthquake motion.
3) The maximum drift angle of wooden house depends on construction condition of junction metallic material in wooden house. Consequently, poor construction of junction metallic material between timber elements in wooden house may significantly affect seismic performance of wooden house against a strong earthquake motion.

ACKNOWLEDGEMENTS

The authors would like to thank the Japan Meteorological Agency and the National Research Institute for Earth Science and Disaster Prevention in Japan for their earthquake ground motion wave data in K-NET and KiK-net systems. Also, the authors would like to thank Mr. Takahashi at Kawashima Construction Co. Ltd. for his cooperation on a wooden house information. This seismic collapsing analysis was conducted by Mr. Reo Mukaide, who was a graduate student at National Institute of Technology, Maizuru College. The authors would like to thank him for his research support and corporation.

REFERENCES

Building Research Institute in Japan. (2016)," The 2016 Kumamoto Earthquake of April 16, 2016", http://iisee.kenken.go.jp/quakes2/20160416kumamoto.html.

Cundall, P. A. and Strack, O. D. L. (1979), "A discrete numerical model for granular assemblies", *Géotechnique*, Vol.29, No.1, 47-65.

Japan Meteorological Agency (20116), http://www.data.jma.go.jp/svd/eqev/data/kyoshin/jishin/1604160125_kumamoto/index.html.

Nakagawa, T., Ohta, M. (2010), "Collapsing process simulations of timber structures under dynamic loading III: Numerical simulations of the real size wooden houses", *Journal of Wood Science,* Vol.56, No.4, 284-292.

National Institute for Land and Infrastructure Management. (2016), "Committee report on cause analysis of seismic building damage in the Kumamoto Earthquake", http://www.nilim.go.jp/english/eindex.htm.

Takatani, T. (2014), "Seismic collapsing analysis of two-story wooden house, Kyo-machiya, against strong earthquake ground motion", *Proceedings of the 2014 International Conference on Geotechnical and Structural Engineering* (CGSE 2014), Hong Kong, China.

Takatani, T. and Nishikawa, H. (2015), "Seismic collapsing analysis of one-story wooden kindergarten structure against strong earthquake ground motion", *Proceedings of the 8th International Conference in Structural Engineering and Construction* (ISEC-8), Sydney, Australia.

Takatani, T. and Nishikawa, H. (2016), "Seismic performance of an old Japanese-style two-story wooden house under a strong earthquake ground motion", *Proceedings of the 3rd Australasian and South-East Asia Structural Engineering and Construction Conference* (ASEA-SEC-3), St-5, ISBN: 978-0-9960437-3-1, Kuching, Sarawak, Malaysia.

Takatani, T. and Nishikawa, H. (2017), "Seismic performance of Japanese-style two-story wooden house against the 2016 Kumamoto Earthquake", *Proceedings of the 2017 World Congress on Advances in Structural Engineering and Mechanics* (ASEM2017), T5F-5, Ilsan (Seoul), Korea.

Watanabe, M., Yamada, K, and Yagi, S. (2003), "Effect of Construction Failure on the strength at Junction Metallic Material for Wooden Structure", *Proceedings of the Architectural Institute of Japan (Tokai Branch)*, No.41, 289-292.

Wikipedia. (2016), https://ja.wikipedia.org/wiki/%E7%86%8A%E6%9C%AC%E5%9C%B0%E9%9C%87_(2016%E5%B9%B4) (in Japanese).